Proc. Natl. Acad. Sci. USA
Vol. 90, pp. 3690–3694, April 1993
Developmental Biology

Two cell-density domains within the *Myxococcus xanthus* fruiting body

(multicellular development/pattern formation/morphogenesis/Myxobacterales)

BRIAN SAGER AND DALE KAISER*

Departments of Biochemistry and Developmental Biology, Beckman Center for Molecular and Genetic Medicine, Stanford University School of Medicine, Stanford, CA 94305

Contributed by Dale Kaiser, January 8, 1993

ABSTRACT **_Myxococcus xanthus_, one of the simplest of multicellular organisms, develops into an organized, multicellular aggregate, called a fruiting body. Examination of the internal structure of the nascent fruiting body showed it to consist of a hemispherical outer domain of densely packed and ordered cells. Inside this dense shell is an inner domain of less ordered cells at 3-fold lower cell density. Single cells move in a bidirectional stream in the outer domain, orbiting the fruiting body throughout development, whereas in the inner domain, cell movement ceases as the fruiting body matures. The fruiting body thus consists of two domains, distinguished from each other by differential cell density, cell arrangements, and cell movements.**

Myxococcus xanthus, a social bacterium, forms a multicellular aggregate upon nutrient starvation, when ≈100,000 cells migrate into a hemispherical mound, the fruiting body (1, 2). Multicellular morphogenesis of the fruiting body precedes a cellular morphogenesis, in which the initially rod-shaped, motile cells that have accumulated within the nascent fruiting body differentiate into spherical, nonmotile myxospores (2).

Electron microscopy of fruiting bodies has revealed aligned arrays of densely packed cells (3, 4); this architecture was assumed to be present uniformly throughout the fruiting body interior. However, interpretations of images of thick sections examined by electron microscopy are complicated by the invasive nature of sample preparation. Moreover, cells migrate to the foci that become fruiting bodies in streams and in spirals (5, 6), which suggests that cell arrangements within the fruiting body might not be homogeneous. To examine the internal architecture of the fruiting body more closely, fluorescence confocal microscopy was employed because it allows nondestructive optical sectioning of thick objects (7). We report here that nascent fruiting bodies consist of an outer hemispherical domain of densely packed and moving cells surrounding an inner domain of nonmoving cells at 3-fold lower cell density.

MATERIALS AND METHODS

Fluorescent Cell Labeling and Fluorescence Measurements. Wild-type cells [strain DK1622 (8)] were grown in CTT broth (9) and harvested in midlogarithmic phase growth. Two hundred fifty microliters of cells at 5×10^8 cells per cm^3 was mixed with 250 μl of 10 μM PKH-2 in 30 mosM diluent A (Zynaxis Cell Science, Malvern, PA; ref. 10). The mixture was incubated at room temperature for 5 min, and then the staining reaction was stopped by addition of 500 μl of a 2% bovine serum albumin solution. The mixture was mixed in a Vortex briefly and incubated at room temperature for 1 min; then cells were washed twice with TPM buffer (9).

For development, labeled cells were concentrated by sedimentation to a density of 5×10^9 cells per cm^3, spotted in 20-μl volumes onto TPM agar (9)-coated microscope slides, and incubated at 33°C in a humid chamber. Fluorescence confocal microscopy was performed with the Phoibos 1000 confocal dual laser scanning system from Molecular Dynamics (Sunnyvale, CA), using a Zeiss Axioscop microscope equipped with a Zeiss Plan-Neofluor objective [40×, 0.75 numerical aperture (n.a.)]. Fluorescence-activated cell sorting was performed as described (11).

Video Microscopy. Video microscopy was performed using a Leitz Labovert inverted microscope equipped with an array of objectives [a Zeiss 2.5× (n.a. 0.08), a Leitz Neofluor 6.3× (n.a. 0.20), a Leitz Phaco 10× (n.a. 0.25), a Leitz Neofluor 25× (n.a. 0.35), and a Leitz Neofluor 40× (n.a. 0.75)] and a Panasonic WV-BD400 CCD video camera. Videographic data were passed through a Panasonic WJ-810 time-date generator, contrast-enhanced by an Argus-10 image processor (Hamamatsu, Middlesex, NJ), and then recorded by a Panasonic TQ-3031F optical disc recorder onto a Panasonic TQ-FH332 optical disc. Image analysis was performed by eye using a Sony PVM-122 black and white video monitor and a Sony UP-3000 video printer. Image acquisition during time-lapse recording was driven by an IBM XT personal computer running custom-written software. When cells were not being videographed, light from the microscope lamp was blocked by a Uniblitz (Vincent Associates, Rochester, NY) VS14 shutter, which was integrated into the microscope's light path and triggered by a Uniblitz T132 shutter driver. Culture temperature was maintained by a Nicholson air stream stage incubator (Nicholson Precision Instruments, Bethesda, MD) and monitored by a YSI telethermometer coupled to a YSI 400 series surface temperature probe (both from Yellow Springs Instrument).

RESULTS

Internal Structure of the Nascent Fruiting Body. To produce fluorescent cells, wild-type *M. xanthus* was labeled with a lipophilic fluorescent probe, PKH-2, which has an excitation peak of 488 nm and an emission peak of 515 nm (ref. 10; see *Materials and Methods*). Cells labeled with PKH-2 at a concentration of 5 μM grew normally; the doubling time of labeled and unlabeled cell cultures was 4.5 h. At this staining concentration, fruiting bodies developed with normal morphology.

The resolving power of probe labeling was measured by mixing freshly labeled and nonlabeled cells in a 1:1 ratio and separating cells in a fluorescence-activated cell sorter (11). Labeled and unlabeled cells fell into discrete populations separated by a median fluorescence intensity difference of 150-fold (Fig. 1*A*). The low-level background fluorescence evident for unlabeled cells may reflect the presence of

The publication costs of this article were defrayed in part by page charge payment. This article must therefore be hereby marked "*advertisement*" in accordance with 18 U.S.C. §1734 solely to indicate this fact.

*To whom reprint requests should be addressed.

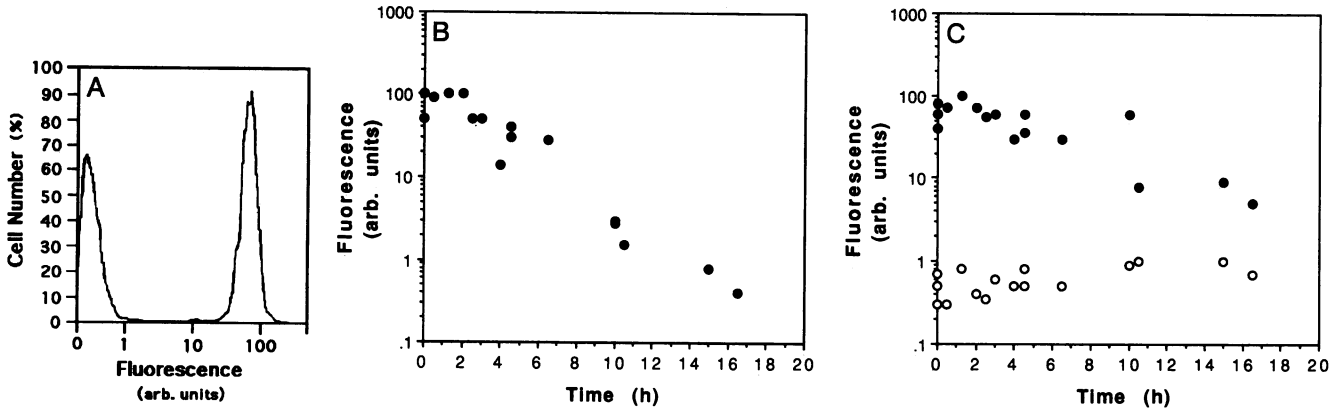

FIG. 1. (*A*) Distribution of fluorescence intensity (indicated in arbitrary units) in a 1:1 mixture of freshly labeled and unlabeled cells. (*B*) Median fluorescence intensity of a population of labeled, growing cells as a function of growth time. (*C*) Median fluorescence intensity of a 1:1 mixture of labeled (●) and unlabeled (○) cells in nonnutrient buffer (i.e., in the absence of growth) as a function of incubation time.

endogenous fluorescent compounds within the cell; *Myxococcus* is known for its high pigment content (1).

The stability of probe labeling was tested in the presence and absence of cell growth. In the presence of cell growth, the probe appeared to be diluted, as indicated by a progressive decrease in the distribution of fluorescence in growing labeled cells (Fig. 1*B*). However, fluorescence fell 100-fold as cell density increased 10-fold, indicating that label dilution was not the only factor responsible for this decrease. In the absence of cell growth, labeled cells exhibited a 10-fold decrease in fluorescence (Fig. 1*C*), accounting for the excess loss of fluorescence seen over dilution by growth. This excess fluorescence loss was not due to probe leakage, however, since the coincubation of an equal number of labeled and nonlabeled cells did not result in an increase in fluorescence among the unlabeled cells as the labeled cells became less fluorescent (Fig. 1*C*).

To examine the internal structure of the fruiting body, wild-type cells were fluorescently labeled and then placed at high density on the surface of a starvation agar plate to initiate development (see *Materials and Methods*). Nascent fruiting bodies were examined by fluorescence confocal microscopy 24 h later, at which time sporulation normally begins (ref. 12; unpublished data). Optical sections at 20 μm above the base (at the top of the fruiting body), at 6 μm above the base, and at the base of a representative fruiting body are shown in Fig. 2. At the top of the fruiting body (Fig. 2*A*), the distribution of fluorescence is rather uniform. However, from the base to 15 μm above the base (roughly three-fourths the height of the nascent fruiting body), the fluorescence distribution is bimodal (Fig. 2 *B* and *C*). Fluorescence at the center of the fruiting body is less intense than at the periphery. Fig. 2*D* shows a gray-scale intensity scan along a diameter of the fluorescence image of Fig. 2*B*; the inner domain averaged a fluorescence intensity at 30% of that within the basal outer domain. Similar results were obtained for 100 wild-type fruiting bodies.

Controls for Fluorescence Quenching. The accuracy with which fluorescence intensity can measure cell density depends on the extent to which intracellular fluorescence is altered by self-quenching. In fact, the calculated cell surface distribution of the label indicates a minimum average intermolecular probe separation of 13 Å, which is well within the 10- to 60-Å range of fluorescence energy transfer (14, 15). However, the observed relationship of fluorescence loss to cell growth argues against self-quenching: As growing labeled cells undergo two population doublings, the minimum average intermolecular separation should increase to at least 52 Å. Since fluorescence energy transfer varies as the inverse sixth power of distance (14), this average separation of proximate label molecules should be great enough to substantially reduce fluorescence energy transfer, resulting in a transient increase in fluorescence intensity. The absence of a transient increase during

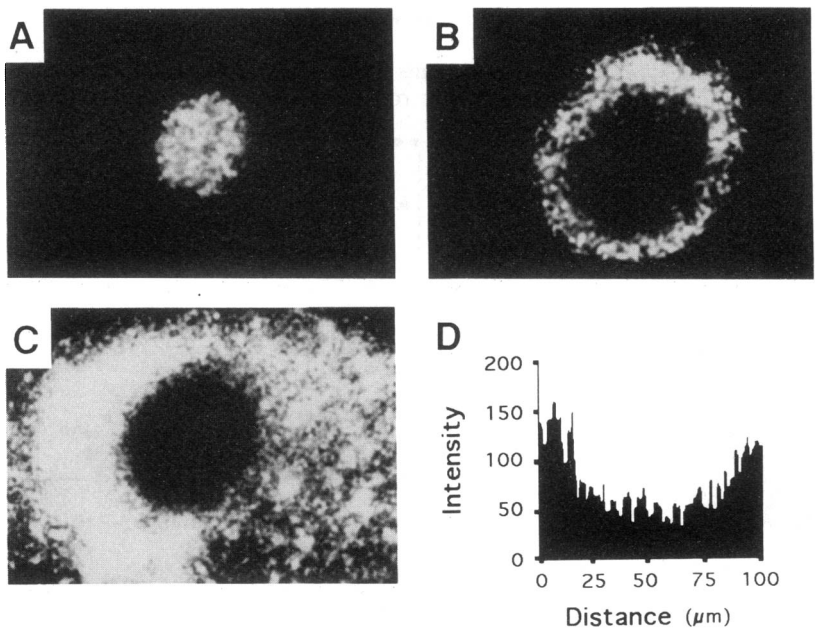

FIG. 2. Fluorescence confocal microscopy of optical sections at 20 μm above the base (*A*), 6 μm above the base (*B*), and at the base (*C*) of a representative wild-type fruiting body at 24 h of development. (*D*) Quantitative gray-scale intensity scan along a diameter of the confocal section shown in *B*.

outgrowth in fluorescence intensity (Fig. 1*B*) argues against significant intracellular quenching of proximate label molecules.

To control directly for the possibility that the low fluorescence of the inner domain was the result of quenching, the concentration of label used to stain cells was progressively decreased from 5 μM to 5 nM. By decreasing the surface density of the label, interactions between PKH-2 molecules should be reduced, and quenching that would alter the fluorescence pattern would diminish. Decreasing the labeling concentration over a 1000-fold range did not alter the (3:1) staining pattern within the fruiting body, though the signal did decrease in intensity, as expected. Thus, there was no indication of intermolecular quenching within the inner domain of the fruiting body.

The accuracy of the estimate of the cell density in the fruiting body interior, as derived from fluorescent images, might be limited by the degree to which label molecules on adjacent cells quench each other's fluorescence. To test this possibility, labeled nonmotile cells were closely packed on nutrient agar scored with grooves whose width approximated the length of cells: With growth, the walls of the grooves should tend to align the cells, which are asymmetric (about 0.5 μm × 6 μm). Indeed, the cell arrangements within such microscopic grooves have been shown to resemble the regular alignment within the nascent fruiting body closely enough to allow the expression of a set of genes dependent upon cell alignment at high cell density (16). If intercellular quenching were to occur within a groove of labeled cells, the center of that groove should appear less intense when examined by fluorescence confocal microscopy. However, when labeled cells in grooves were examined by bright-field and fluorescence confocal microscopy, the fluorescence image was, if anything, slightly more intense in the center, reflecting perhaps a greater cell density due to a higher degree of cell alignment in the center of the groove (compare Fig. 3 *A* and *B*).

We have also labeled cells with a rhodamine-like probe, PKH-26; the excitation peak (551 nm) and emission peak (567 nm) of this probe differ from those of PKH-2, yet the fluorescence pattern remained identical (data not shown). It is therefore unlikely that the fluorescence pattern in the inner domain is due to a localized fluorescence-absorbing substance, unless such a substance equally absorbed light of different wavelengths.

Finally, to confirm that the difference in fluorescence intensity corresponds to a difference in cell density between two domains within the fruiting body, fruiting bodies were also examined by bright-field microscopy. Fifty fruiting bodies containing labeled cells were observed in the same focal plane by confocal and bright-field microscopy. In all cases, identical topologies were observed (compare Fig. 4 *A* and *B*).

Cell Densities in the Inner and Outer Domains. Since the outer domain (at the base of a fruiting body) appears to contain maximally aligned cells (4, 16), its cell density can be calculated by approximating each cell's shape as a cylinder with radius (r) of 0.50 μm and length (l) of 6.0 μm (unpublished data), where the volume of a single cell, $\pi r^2 l$, is 4.7 μm^3, and determining the maximum number of 4.7 μm^3 cylinders that can be packed into 1 cm^3. Assuming the maximum possible cell density of 2×10^{11} cells per cm^3 is present within the outer domain, since the cell density in the inner domain is ≈30% of that in the outer domain, it would contain ≈6×10^{10} cells per cm^3.

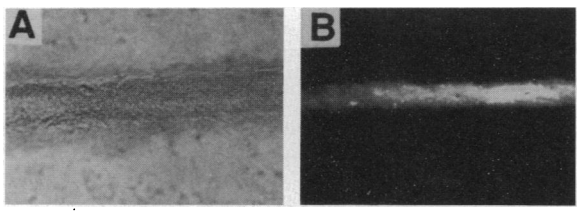

FIG. 3. Bright-field inverted microscopic image (*A*; ×25) and fluorescence confocal image (*B*; ×40) of labeled cells (strain DK4170) closely packed on nutrient agar scored with grooves.

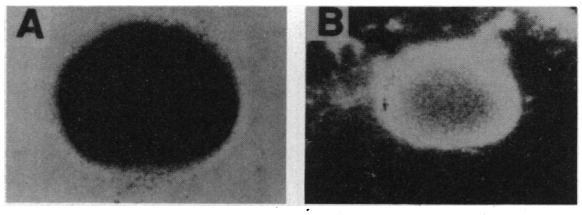

FIG. 4. Bright-field inverted microscopic image (*A*; ×25) and fluorescence confocal microscopic image (*B*; ×40) of the same fruiting body in the same focal plane.

Cell Orientations in the Inner and Outer Domains. Wild-type cells (strain DK1622) were allowed to develop on agar-coated slides for 24 h and the bases of fruiting bodies were then examined with inverted bright-field optics. At high optical magnification, arrays of dark elongate spots are present within the fruiting body. The regular arrangements of these elongate spots are likely to represent either an ordered arrangement of individual cells or a moiré pattern produced by the interaction of light rays with an ordered array of cells. Cells are known to be arranged in aligned parallel arrays within the fruiting body (3, 4, 16). The density of spots at the base of the fruiting body was directly measured. In the outer region of the fruiting body there was one spot per μm^2, whereas the center of the fruiting body showed one spot per 2.4 μm^2. This ratio of 1:2.4 in spot density is consistent with the ratio of cell density obtained from fluorescence measurements (Fig. 2*D*).

The orientation of these elongate spots was examined at high magnification. The complement of the angle between a radius drawn from the center of the fruiting body to the center of a spot and the long axis of that spot (the tangential deviation) was measured for each spot. Tangential deviation was measured for 300 randomly chosen spots along the fruiting body base of three wild-type (strain DK1622) fruiting bodies. The tangential deviation was low in the outer domain of the fruiting body and abruptly increased in the inner domain of the fruiting body, indicating a higher degree of cellular order in the outer domain than in the center (Fig. 5). A similar pattern was qualitatively observed for >1000 fruiting bodies.

Cell Movements in the Outer Domain. Videographic analyses show that rod cells are present and move primarily

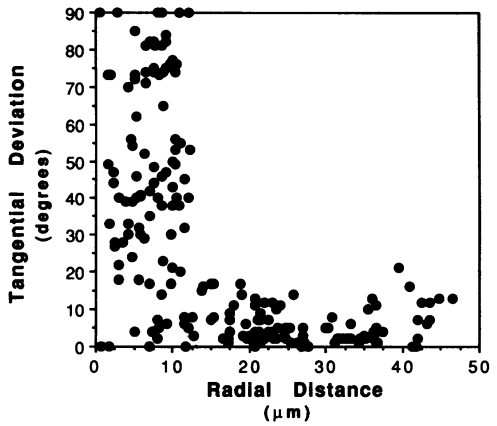

FIG. 5. Tangential deviation of a spot as a function of radial distance from the center of the fruiting body (n = 199).

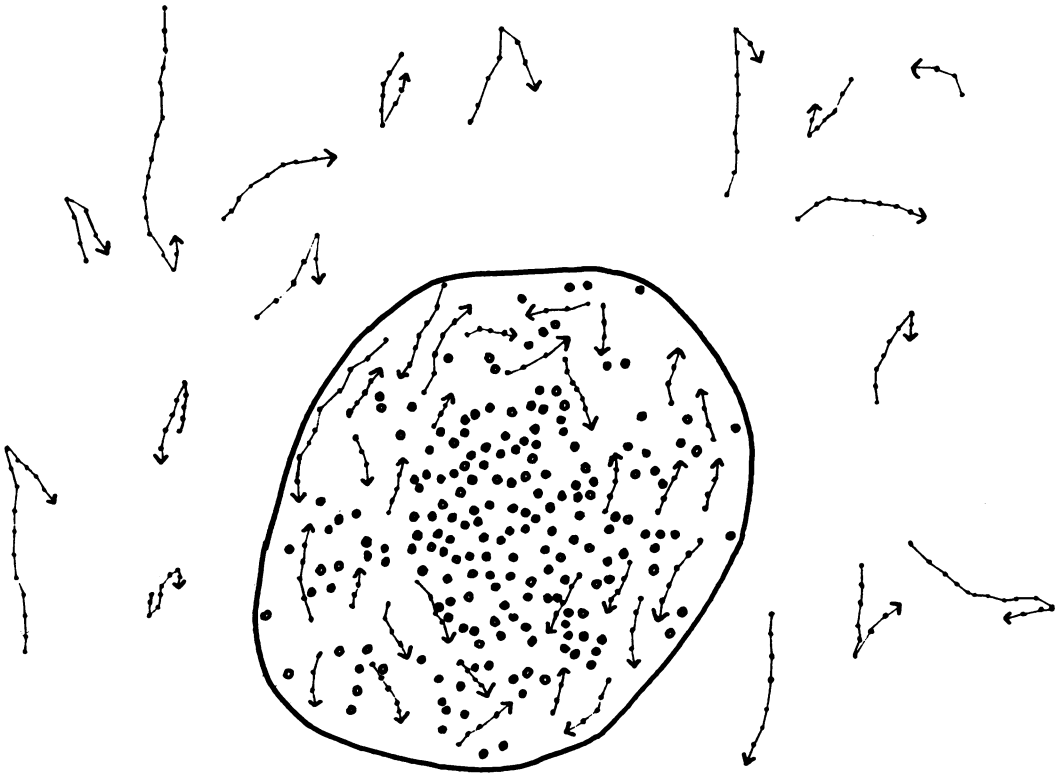

FIG. 6. The paths of randomly chosen single cells, tracked frame-by-frame by the progressive displacements of their centers of area, are shown at the base of a representative wild-type fruiting body at 40 h of development. The time between frames is 20 s. Tiny solid dots (•) represent successive positions of the moving rod cells; open circles (○) depict nonmoving spherical cells. Arrows represent the directions of cell movement. The solid line represents the fruiting body perimeter.

within the outer domain of the fruiting body. Cell movements near and within randomly chosen fruiting bodies were measured at 40 h of submerged culture development (see *Materials and Methods*), since before this time aggregating cells were moving in streams that were too dense to allow for single-cell analysis.

The paths of single cells, tracked frame-by-frame by the progressive displacements of their centers, are shown for a representative fruiting body in Fig. 6. Outside of the fruiting body, cells reversed frequently; when 17 randomly chosen cells were tracked, 14 reversals were detected in a total of 57 cell-min, yielding an average reversal frequency of 0.3 reversal per min, a frequency comparable to that measured by Blackhart and Zusman (18). Within the fruiting body, 31 randomly chosen cells were followed at the base of the outer domain; no reversals were detected in a total of 56 cell-min. These cells moved in paths roughly circumferential to the fruiting body perimeter, forming two cell streams, one moving clockwise, the other counterclockwise, in roughly equal proportions (Fig. 6). In contrast, in the inner domain, where the cells had the high optical refractivity and spherical morphology characteristic of spores, cell movement was not detected. Thus the outer and inner domains of the fruiting body can also be distinguished by differential cell movement.

No reversals were observed for cells in the outer domain of the fruiting body, yet in Fig. 6, the mean path length of these cells, 1.5 cell-min, is lower than the mean path length of cells followed outside the fruiting body, 2.1 cell-min. Might this difference have eliminated the chance of observing reversals in the outer domain? Examination of the paths of cells outside of the fruiting body (Fig. 6) showed that number of reversals accumulated linearly in time, following the equation $R = 0.3T$ (with a regression coefficient = 0.91), where R is the accumulated number of reversals, and T is time, in min. The slope of the line, 0.3, is the probability of a cell reversal, in reversals per min. Inside the fruiting body, were cells to have the same reversal frequency as cells outside, five reversals would have been expected. Thus, the mean path length of cells tracked in the outer domain is sufficient to allow the detection of reversals had they occurred. However, none was detected.

The data of Fig. 6 do represent the general behavior of cells in developing fruiting bodies. In three other experiments, fruiting bodies were chosen at random, and reversal frequencies were measured for cells whose path lengths exceeded 1.5 cell-min. Cells outside of these fruiting bodies showed an overall average of 0.29 reversal per min (n = 1012 cell-min), whereas cells within the outer domain of the fruiting bodies reversed on average 0.09 time per minute (n = 474 cell-min).

DISCUSSION

We have shown that the fruiting body contains an outer domain of relatively high cell density and cell order and a relatively less dense and less ordered inner domain (Figs. 2 and 5). Cell movement within the fruiting body is domain-specific. Cells in the outer domain move in concentric clockwise and counterclockwise streams, whereas no cell movement was detected in the inner domain, which contains cells displaying the optical refractivity and spherical morphology characteristic of spores (Fig. 6). The circling, infrequently reversing paths of single cells in the outer domain of the fruiting body contrast with the more frequent reversals of growing cells (18) and of cells outside nascent fruiting bodies and are consistent with spiral arrangements of cells detected within the *Myxococcus* fruiting body by electron microscopy (4).

Patterns of spiral cell movements are found in the aggregation of several Myxobacteria (5, 6, 19) and in the aggregation of the eukaryotic slime mold *Dictyostelium discoideum* (20). In *Dictyostelium*, plane waves propagate within

the developing slug (21); these waves are likely to be organized by the chemotactic responses of cells to extracellular cAMP, which has properties of a morphogenic signal in *Dictyostelium* (22, 23). In *M. xanthus*, C factor, a 17-kDa protein, acts as a short-range morphogenic signal (13, 17). C factor signaling is restricted to the outer domain of the *Myxococcus* fruiting body (unpublished data). Based on its signaling properties and its spatial distribution within the fruiting body, C factor is likely to be modulating the motility patterns of cells in the outer domain.

We thank research colleagues at Stanford and Dr. David Zusman (University of California at Berkeley) for helpful discussions and criticism and the Hassleblad Foundation for an optical equipment grant. B.S. was supported by a National Science Foundation predoctoral fellowship. Research was supported by American Cancer Society Grant NP-772.

1. Rosenberg, E., ed. (1984) *Myxobacteria, Development and Cell Interactions* (Springer, New York).
2. Shimkets, L. J. (1990) *Microbiol. Rev.* **54**, 473–501.
3. Kaiser, D., Kroos, L. & Kuspa, A. (1985) *Cold Spring Harbor Symp. Quant. Biol.* **50**, 823–830.
4. O'Conner, K. A. & Zusman, D. R. (1989) *J. Bacteriol.* **171**, 6013–6024.
5. Reichenbach, H. (1965) *Ber. Dtsch. Bot. Ges.* **78**, 102–105.
6. Reichenbach, H. (1966) in *Encyclopedia Cinematographica*, ed. Wolf, G. (Inst. Wissenschaftlichen Film, Göttingen, Germany), pp. 557–578.
7. Brakenhoff, G. J., Van Der Voort, H. T. M., Van Spronsen, E. A. & Nanninga, N. (1989) *J. Microsc.* **153**, 151–159.
8. Kaiser, D. (1979) *Proc. Natl. Acad. Sci. USA* **76**, 5952–5956.
9. Kroos, L., Kuspa, A. & Kaiser, D. (1986) *Dev. Biol.* **117**, 252–266.
10. Horan, P. K. & Slezak, S. E. (1989) *Nature (London)* **340**, 167–168.
11. Russo-Marie, F., Roederer, M., Sager, B., Herzenberg, L. A. & Kaiser, D. (1993) *Proc. Natl. Acad. Sci. USA*, in press.
12. LaRossa, R., Kuner, J., Hagen, D., Manoil, C. & Kaiser, D. (1983) *J. Bacteriol.* **153**, 1394–1404.
13. Kim, S. K. & Kaiser, D. (1990) *Cell* **61**, 19–26.
14. Förster, T. (1948) *Ann. Phys. (Leipzig)* **2**, 55–75.
15. Stryer, L. & Haugland, R. P. (1967) *Proc. Natl. Acad. Sci. USA* **58**, 719–726.
16. Kim, S. K. & Kaiser, D. (1990) *Science* **249**, 926–928.
17. Shimkets, L. J. & Rafiee, H. (1990) *J. Bacteriol.* **172**, 5299–5306.
18. Blackhart, B. D. & Zusman, D. R. (1985) *Proc. Natl. Acad. Sci. USA* **82**, 8767–8770.
19. Stephens, K. & White, D. (1980) *FEMS Microbiol. Lett.* **9**, 189–192.
20. Durston, A. J. (1974) *Dev. Biol.* **37**, 225–235.
21. Siegert, F. & Weijer, C. J. (1992) *Proc. Natl. Acad. Sci. USA* **89**, 6433–6437.
22. Tomchik, K. & Devreotes, P. N. (1981) *Science* **212**, 443–446.
23. Devreotes, P. N. (1989) *Science* **245**, 1054–1058.